# Frozen-State Storage Stability of a Monoclonal Antibody: Aggregation is Impacted by Freezing Rate and Solute Distribution

MARIA A. MILLER,[1] MIGUEL A. RODRIGUES,[1] MATTHEW A. GLASS,[1] SATISH K. SINGH,[2] KEITH P. JOHNSTON,[1] JENNIFER A. MAYNARD[1]

[1]Department of Chemical Engineering, University of Texas at Austin, Austin, Texas 78712

[2]Pfizer Inc., Biotherapeutics Pharmaceutical Sciences, Chesterfield, Missouri 63017

*Received 27 August 2012; revised 8 January 2013; accepted 22 January 2013*

*Published online 8 February 2013 in Wiley Online Library (wileyonlinelibrary.com). DOI 10.1002/jps.23473*

**ABSTRACT:** Freezing of protein solutions perturbs protein conformation, potentially leading to aggregate formation during long-term storage in the frozen state. Macroscopic protein concentration profiles in small cylindrical vessels were determined for a monoclonal antibody frozen in a trehalose-based formulation for various freezing protocols. Slow cooling rates led to concentration differences between outer edges of the tank and the center, up to twice the initial concentration. Fast cooling rates resulted in much smaller differences in protein distribution, likely due to the formation of dendritic ice, which traps solutes in micropockets, limiting their transport by convection and diffusion. Analysis of protein stability after more than 6 months storage at either $-10^{\circ}$C or $-20^{\circ}$C [above glass transition temperature ($T'_g$)] or $-80^{\circ}$C (below $T'_g$) revealed that aggregation correlated with the cooling rate. Slow-cooled vessels stored above $T'_g$ exhibited increased aggregation with time. In contrast, fast-cooled vessels and those stored below $T'_g$ showed small to no increase in aggregation at any position. Rapid entrapment of protein in a solute matrix by fast freezing results in improved stability even when stored above $T'_g$. © 2013 Wiley Periodicals, Inc. and the American Pharmacists Association J Pharm Sci 102:1194–1208, 2013

**Keywords:** biopharmaceuticals characterization; excipients; formulation; protein aggregation; protein formulation; stability

## INTRODUCTION

Proteins, especially therapeutic monoclonal antibodies, have received considerable attention from the biotechnology industry because of the rapidly increasing market size and corresponding advances in antibody engineering and manufacturing technologies.[1–3] The ability to store bulk quantities of these large macromolecules for significant periods of time while maintaining native protein conformation and full activity remains a major technical challenge.[4] Bulk protein solution storage in the frozen state is generally preferred over liquid storage, as the solid state confers increased stability and shelf life decreases the risk of microbial contamination and growth and eliminates foaming during transport.[5] However, both freezing and thawing processes and storage temperatures, if not properly selected, have been shown to adversely affect protein stability.[6–8] Typically, small-scale studies (<5 mL) are utilized to optimize the formulation, including the buffer composition, pH, ionic strength, and for selection of cryoprotectants. Small volume minitanks of the type used in this work are often used as representative containers for long-term stability studies to determine shelf life for bulk protein solution stored in large tanks.[9] However, these small volume scaled-down freeze–thaw and stability studies, used to predict the behavior of larger volumes, largely ignore the direct impact of freezing rates and subsequent protein distribution on long-term protein stability.[7,10–14]

**Abbreviations used:** FCM, freeze-concentrated matrix; HMMS, high-molecular-mass species; SEC, size-exclusion chromatography; $T'_g$, glass transition temperature

*Correspondence to*: Keith P. Johnston (Telephone: +512-471-4617; Fax: +512-471-7060; E-mail: kpj@che.utexas.edu); Jennifer A. Maynard (Telephone: +512-471-9188; Fax: +512-471-7060; E-mail: maynard@che.utexas.edu); Satish K. Singh (Telephone: +636-247-9979; Fax: +860-686-7786; E-mail: satish.singh@pfizer.com)

Miguel A. Rodrigues' s present address is Department of Chemical Engineering, Instituto Superior Técnico, Lisboa, Portugal.

Journal of Pharmaceutical Sciences, Vol. 102, 1194–1208 (2013)

Freezing changes the protein distribution in the volume being processed. Unless a solute possesses crystallographic similarities to water crystals, the growing ice front will preferentially take up water molecules from the ice–liquid interface; thus, increasing the concentration of the solutes in the liquid near this interface. The concentration profile of solutes entrapped between the ice crystals results from a balance between the ice front velocity versus the rates of diffusive and convective transport of solute away from the interface.[15–17] Solute exclusion from the nucleating ice domains is influenced by differences in interfacial energy as well as the crystal lattice structure,[15] whereas solute inclusion results when the ice growth rate exceeds the solute mass transfer rate away from the advancing ice front.[18,19] After freezing is complete, the solute distribution may vary significantly throughout the frozen mass, a process referred to as freeze concentration or concentration polarization.[10,20] The solute distribution is thus determined by the cooling process, which determines the freezing rate or ice front velocity and by the dimensions of the system. For the same heat-transfer (cooling) rate, a small vessel will show a less polarized distribution than a large vessel simply because the ice front will progress faster in the former, creating smaller crystals, thus distributing the freeze-concentrated matrix (FCM) over a greater geometric area. A detailed analysis of the spatial distribution of solutes (lysozyme and trehalose) in frozen samples by confocal Raman microspectroscopy supports the above general description.[21] However, this analysis also showed that for a rapidly propagating ice front, inclusions containing high concentrations of solutes were also to be found dispersed in the ice phase. Apart from these inclusions, the ice phase itself was not found to be of pure water but containing low concentrations of the solutes with a higher degree of entrapment of lysozyme than trehalose.[21]

We recently reported a study relating freezing rates in a 2.5 cm diameter, 50 mL cylindrical stainless steel vessels to the immunoglobulin G (IgG) monoclonal antibody concentration profile in ice.[19] At the slow freezing rates produced by stagnant air freezers, solutes, including the protein and trehalose, were found to freeze concentrate at the same ratio toward the bottom and center of the vessel, as a consequence of natural convection.[19] At faster freezing rates induced by forced convection of air or liquid coolant, ice dendrites became more prevalent. These are protuberances of ice formed in the supercooled liquid layer immediately ahead of the interface.[19] During freezing, the ice dendrites increase drag forces and disrupt natural convection flow patterns, thereby attenuating solute transport away from the ice front.[15,16,20,22–24] Thus, formation of ice dendrites during fast freezing enhances solute entrapment (in FCM), limiting macroscopic solute concentration polarization within the ice.[22]

We have also recently reported on the ability of trehalose to crystallize from the frozen state during long-term storage at temperatures above the $T'_g$ (glass transition temperature of the frozen matrix). The crystallization of trehalose resulted in loss of cryoprotection leading to significant aggregation of the IgG in storage at −20°C, but only minor to no aggregation at −10°C. Mobility on storage above $T'_g$ allows trehalose to crystallize. It is hypothesized that the mobility also enables the protein in the FCM to either aggregate from the ice-interface-induced denaturation state by interacting with neighboring unfolded molecules or to recover to its properly folded monomeric state. The balance between these competing rates leads to the observation of aggregation at −20°C but not at −10°C.[25]

The primary objective of this study was to determine the effect of the freezing process and subsequent frozen-state storage on the stability of an IgG2 therapeutic monoclonal antibody, thus relating the stability to the concentration profile in the frozen state. This study builds upon our previous reports relating the protein concentration profile within solid ice to freezing rates and ice dendrite morphology,[19] and frozen-state protein aggregation to cryoprotectant crystallization.[25] The formation of dendrites has been suggested to favor protein stability.[16,23] However, the relationship among freezing rates, dendrite formation, protein concentration profiles, and protein stability in a well-defined geometry has not been reported.

Frozen IgG2 samples were prepared in 50-mL stainless steel cylindrical vessels using either fast or slow freezing rates to −20°C, as previously described.[19] The fast freezing rate was produced by immersing the vessel in a liquid coolant solution of water and ethanol, whereas the slow freezing rate was produced by placing the vessel in stagnant air within a freezer.[19] The fast freezing rate was shown to prevent significant solute polarization, whereas the slow freezing rate produced ∼1.5–2× differences in protein concentration near the center and bottom of the tank, as measured in ice cores extracted from the matrix.[19] Replicate frozen tanks from each freezing condition were stored at temperatures of −10°C, −20°C, and −80°C. After storage for 2–12 months, small cores were removed from the ice at various heights and distances from the center. After thawing the core samples, the protein concentration, conformation, and presence of high-molecular-weight aggregates were assessed.

Slow freezing, when followed by storage at temperatures above $T'_g$, resulted in the expected formation of aggregates.[24] However, surprisingly, fast freezing followed by storage at any temperature above or

below $T'_g$ did not result in aggregation. The vessels frozen at fast freezing rates retain a uniform solute distribution within the FCM. In contrast, slow freezing results in concentration gradients of protein (and other excipients as shown in our earlier study[19]). The degree of aggregation in the slow-cooled tanks correlated with the local protein concentration, which both varied with radial and axial positions within the tank. Our results show that the higher mobility of solute and protein during storage above the $T'_g$ facilitates aggregation as compared with samples stored at temperatures below the $T'_g$.[25] However, distributions of ice and solute created during cooling also impacts the outcome after storage. We hypothesize that solute that is well distributed in interdentritic spaces due to fast cooling apparently has less ability to crystallize and thus provides greater protection to the protein even when stored above $T'_g$. Overall, minimizing concentration gradients and protein mobility within the frozen protein mass by increasing the freezing rate and decreasing the storage temperature below the formulation $T'_g$ is expected to increase protein stability.

A fundamental understanding of protein stability during long-term storage helps to address practical engineering challenges in large-scale protein storage.[26,27] From a manufacturing perspective, analysis of freezing profiles on protein stability in large-scale storage vessels (on the order of 300 L) is impractical.[10] Therefore, small-scale models (e.g., minitanks or vessels of the type used in this work) are commonly used as surrogates to study stability behavior during processing as well as storage.[10,20] Small-scale models are used in long-term stability studies to determine shelf life for bulk protein substance held frozen in large-scale vessels.[9] For these long-term studies, these small-scale model tanks are generally simply placed in the appropriate freezer with no control on the freezing rate. This work represents the first time that these small-scale models have been analyzed in detail for their ability to represent phenomena occurring in large commercial tanks. The work also examines the impact of processing (freezing) rate on the outcome of long-term storage of proteins. To our knowledge, this aspect has never been studied before with the published literature primarily devoted to impact of processing on outcome of freeze–thaw cycling.[14]

This work focuses on the impact of freezing process on the outcome of long-term storage in small-scale models. By working with small samples, we have minimized the impact of the thaw process because the thaw times are minimal. In large-scale systems, the thaw process also becomes important for the outcome, both from the process time involved and whether the thaw is carried out with or without mixing.[4,28] The thaw process therefore represents another significant difference between large commercial systems and the small-scale models used to represent them.

## MATERIALS AND METHODS

### Materials

The IgG2 mAb solution was donated by Pfizer, Inc. (Chesterfield, Missouri), at 20 mg/mL in a 20 mM histidine–HCl buffer at pH 5.5 with 84 mg/mL α,α-trehalose dihydrate, 0.1 mg/mL disodium edetate dihydrate, and 0.2 mg/mL polysorbate 80. Additional α,α-trehalose dihydrate was purchased from Mallinckrodt Baker (Phillipsburg, New Jersey). Additional L-histidine and L-histidine hydrochloride monohydrate were purchased from Fisher Scientific (Fair Lawn, New Jersey), disodium edetate dihydrate was purchased from Spectrum (New Brunswick, New Jersey), and polysorbate 80 was purchased from J.T. Baker Inc. (Phillipsburg, New Jersey). The IgG2 is very stable in the histidine buffer solution listed above, showing very minor changes in quality attributes (aggregation, oxidation, deamidation, and subvisible particle formation) over at least 4 years at 2°C–8°C (data not shown).

### Freezing and Storage of Small Vessels

Electropolished stainless steel (SS316L) minitanks with a 60 mL nominal volume, 5 cm internal diameter, and 7.5 mm wall thickness with 6 mm thick stainless steel lids were sealed by three bolts that compress an o-ring. A 50 mL solution of the 20 mg/mL IgG2 solution was added to each tank after filtration through a 0.2 μm sterilizing-grade filter. Once the protein solution was added, the minitank was sealed and frozen either in a stagnant air freezer or by immersion in a water–ethanol mixture at −20°C, as reported previously.[19] The tanks frozen in the stagnant air freezer were placed inside the −20°C freezer (Scientemp Corporation, Adrian, Michigan; model 45-01A) on top of three polyvinyl chloride (PVC) plugs to avoid direct contact between the bottom surface of the container and the freezer shelf. The liquid-cooled tanks were immersed in an ethanol bath maintained at −20°C by a cooling-circulator PolyScience Controller (Niles, Illinois; model 1197). Temperature profiles in the tanks in these configurations have been presented by us previously.[19]

After 24 h, the frozen tanks were transferred to a −10°C freezer (GE, Fairfield, Connecticutt; model TAX10SNTDRWH), a −20°C freezer (Scientemp Corporation; model 45-01A), or a −80°C freezer (Puffer Hubbard, Thermo Scientific, Waltham, Massachusetts) for long-term storage. An equal number of replicate tanks, both stagnant air cooled or liquid cooled were harvested after 70, 170, 270, and 360 days

of storage at −10°C, 190 and 230 days at −20°C, and 190 and 360 days at −80°C.

### Ice Harvesting

After removing the tank from the freezer, the tank was left to warm for 10–15 min at room temperature to facilitate removal of the ice block, whereas a stainless steel plate (>10 cm in diameter) was cooled in a dry ice bath, and the band saw blade (Delta ShopMaster, Delta PEC, Anderson, South Carolina) was cooled using a piece of solid dry ice. The ice block was removed from the tank and cut axially into five disk slices. The thin top and bottom slices (~3 mm thick) were discarded as the thawing necessary to remove the ice block from the vessel compromised their position-specific profiles. The remaining three slices (~7 mm thick each) were placed on the cooled plate, where three samples (each ~0.5–1 mL) were cored using commercially available stainless steel dies (either 0.2 or 0.5 cm in diameter) from each slice; three near the outer radius ($R_0 \sim 2.5$ cm) and three halfway between the center and the outer radius ($r \sim 1.5$ cm), both using the smaller die and one in the center using the larger die. After each sample melted, 10 μL of a 0.3-wt % sodium azide solution was added to prevent bacterial growth before analyzing the protein concentration and assessing its aggregation state. Tanks stored at −20°C for 230 days were allowed to thaw at refrigerated conditions overnight within the stainless steel minitank itself to obtain an assessment of the "global" stability of the material. Once the entire 50 mL solution was thawed, 500 μL of the 0.3-wt % sodium azide solution was added and six individual 1-mL samples were removed from each tank. All thawed solutions were stored at 4°C, and further analysis was completed between 1 and 15 days after melting. [Note: sodium azide could potentially have an impact on the oxidation behavior of the IgG2 mAb. However, forced degradation and long-term studies on the mAb have shown no correlation between oxidation and aggregation levels (data not shown).]

As we have previously discussed,[19,29] the coring method described above to determine solute concentrations at different positions provides a macroscopic value that is dependent on the core dimensions. An ice core includes a combination of ice crystals as well as frozen solute matrix or FCM. After melting, the pure ice fraction dilutes the solute fraction, lowering the solute concentration relative to that in the actual FCM between the ice crystals. Thus, this is a macroscopic cryoconcentration value that provides a measure of the extent of solute movement or solute polarization occurring before the completion of freezing process. It is therefore a measure of the heterogeneity introduced into the system by the processing conditions applied. The phrases "macroscopic cryoconcentration," "solute polarization," or "concentration polarization" are used interchangeably in the text and should be considered from the above perspective when applied to the frozen matrix. The cryoconcentration measured in this work therefore is a macroscopic measurement. The true or microscopic cryoconcentration of solutes in the FCM between the ice crystals will be given by the phase or state diagram for the system and theoretically equal the maximal freeze concentration.[30] However, nonequilibrium processing will result in a cryoconcentration level in the FCM lower than this theoretical maximum.

### Measurement of Protein Concentration

After fourfold dilution of each sample in histidine–HCl buffer with 84 mg/mL trehalose, protein concentrations were measured versus a buffer blank by absorbance at 280 nm. This was performed in triplicate on a 96-well Costar UV transparent plate (model #3635) using a μQuant detector (Bio-Tek Instruments Inc., Winooski, Vermont). To calculate sample concentrations, a calibration curve was prepared with protein of known concentration, ranging from 0 to 4 mg/mL and yielding an $R^2$ value greater than 0.99. These values were confirmed at a secondary location (Pfizer Inc.) using a similar UV absorption technique and an extinction coefficient of 1.43 mg/(mL cm). Each core sample was diluted upon melting by ~10% from the addition of sodium azide to prevent bacterial growth and water condensing from the atmosphere. The local relative concentration $C/C_0$ is determined as the measured sample concentration divided by the initial prefreeze concentration, $C_0 = 20$ mg/mL.

### Measurements of Protein Conformation

An intrinsic tryptophan fluorescence assay, in which changes in emission wavelength indicate changes in the local solvent environment surrounding tryptophan residues, was used to monitor the protein conformation after frozen storage. First, the wavelengths corresponding to the maximum emission for fully folded and fully unfolded protein were determined, using native protein and protein equilibrated with 8 M urea as denaturant at a 5 mg/mL protein concentration. Next, a standard unfolding curve for urea-denatured IgG2 was determined based on the ratio of the emission intensities at these two wavelengths, using a series of IgG2 protein samples at 5 and 10 mg/mL, with urea concentrations ranging from 0 to 10 M. After a 1-h equilibration, the ratio of emission intensities at the maximum emission wavelength for fully unfolded protein (350 nm) to the maximum emission wavelength for folded protein (335 nm) was used to determine the percent unfolding (Fig. 1).[31] For test samples, 100 μL of each sample was added to a single well in a UV-transparent 96-well plate (Costar). The sample was excited at 295 nm, a wavelength specific

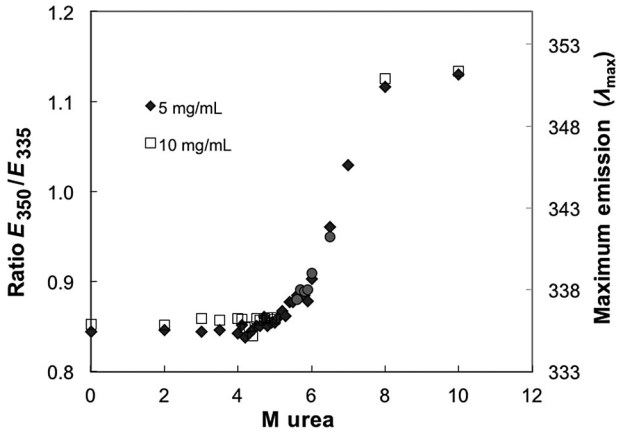


**Figure 1.** Increase in tryptophan fluorescence as a function of antibody urea denaturation. Purified IgG2 antibody was equilibrated with the concentration of urea indicated. The change in tryptophan fluorescence is shown as the maximum emission wavelength (○) and the ratio of the emission intensities at 350 and 335 nm (5 ♦ or 10 mg/mL □).

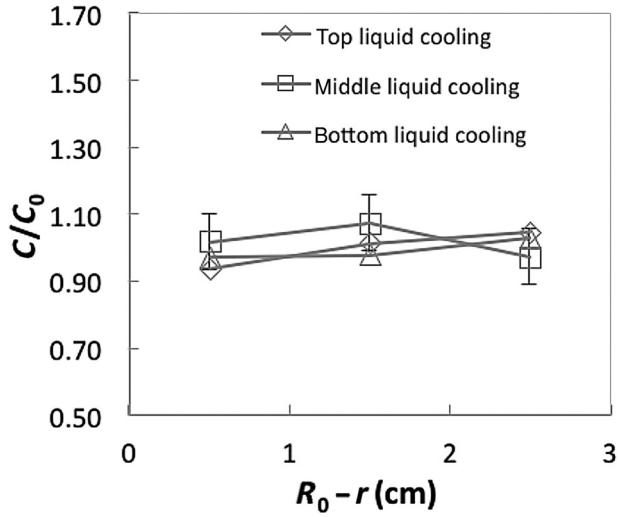


**Figure 2.** Fast cooling effects on concentration gradients as a function of radial position within the vessel. The average protein concentration was measured after ice sampling at various heights and radii from the outside to the center of the tank ($R_0 = 2.5$ cm). The data shown is averaged for all tanks, stored at any temperature for various amounts of time between 70 and 360 days after fast cooling.

for the aromatic tryptophan side chain, and the emission recorded at 1 nm increments between 310 and 380 nm on a SpectraMax M5 instrument (Molecular Devices, Sunnyvale, California). The ratio of observed signal intensities at the two wavelengths ($E_{350}/E_{335}$) was used as a measure of unfolding.

### Measurement of Aggregates

The presence of large particulate aggregates was assessed using optical density at a wavelength of 350 nm measured with a SpectraMax M5 instrument (Molecular Devices).[32] The percent of high-molecular-mass species (HMMS) within each sample (detectable by chromatography) was measured in triplicate using size-exclusion high performance liquid chromatography (SEC-HPLC). Before the analysis, the samples were filtered through a 0.22 μm polyvinylidene difluouride filter. The SEC-HPLC was conducted using on a G3000SWXL column (300 × 7.8 mm$^2$; Tosoh Bioscience LLC, King of Prussia, Pennsylvania), in a 50 mM sodium phosphate buffer at 1.0 mL/min. A sample volume of 20 μL was injected and the elution was tracked at 214 nm through a UV detector. In house, a reference standard was injected before (3×), after every 10 samples (1×), and at the end (1×) of each chromatography batch run. Peak area for the reference standard runs was monitored and tracked overtime to confirm system suitability and eliminate any impact of column or instrument drift on performance. The monomer eluted after ~21 min with the HMMS eluting between 18 and 21 min, depending on their size (see Ref. 25 for representative chromatograms). Results are reported as total %HMMS and incorporate primarily dimeric and some higher order species. Results within 0.2% of each other are not considered significantly different.

Note that because of the intensive processing required to produce the samples and cores and the inability to avoid extraneous contamination, subvisible particulate matter was not measured on these samples. However, the IgG2 mAb in the histidine–trehalose formulation is not particularly susceptible to particle formation on freeze–thaw, especially through a single cycle, as was the case in this study. The incremental number of particles formed after one cycle of freeze–thaw is very small (see Fig. 2f in Ref. 33). In fact, for the same mAb in the same tanks, Barnard et al.[33] had to change the buffer to phosphate-buffered saline to get any significant levels of particle formation on freeze–thaw cycling.

## RESULTS

### Protein Concentration Profile in the Ice

Protein concentration profiles measured for various cores in the top, middle, and bottom ice samples reveal differences for the slow versus fast freezing rates, as has been reported previously.[19] Fast (liquid cooled) freezing resulted in little to no concentration polarization, as measured by our core sampling technique (data not shown). The concentration profiles at particular locations were therefore averaged over all storage times and are plotted in Figure 2. The relative local concentrations, (the measured sample concentration normalized by the initial tank concentration),

 DOI 10.1002/jps

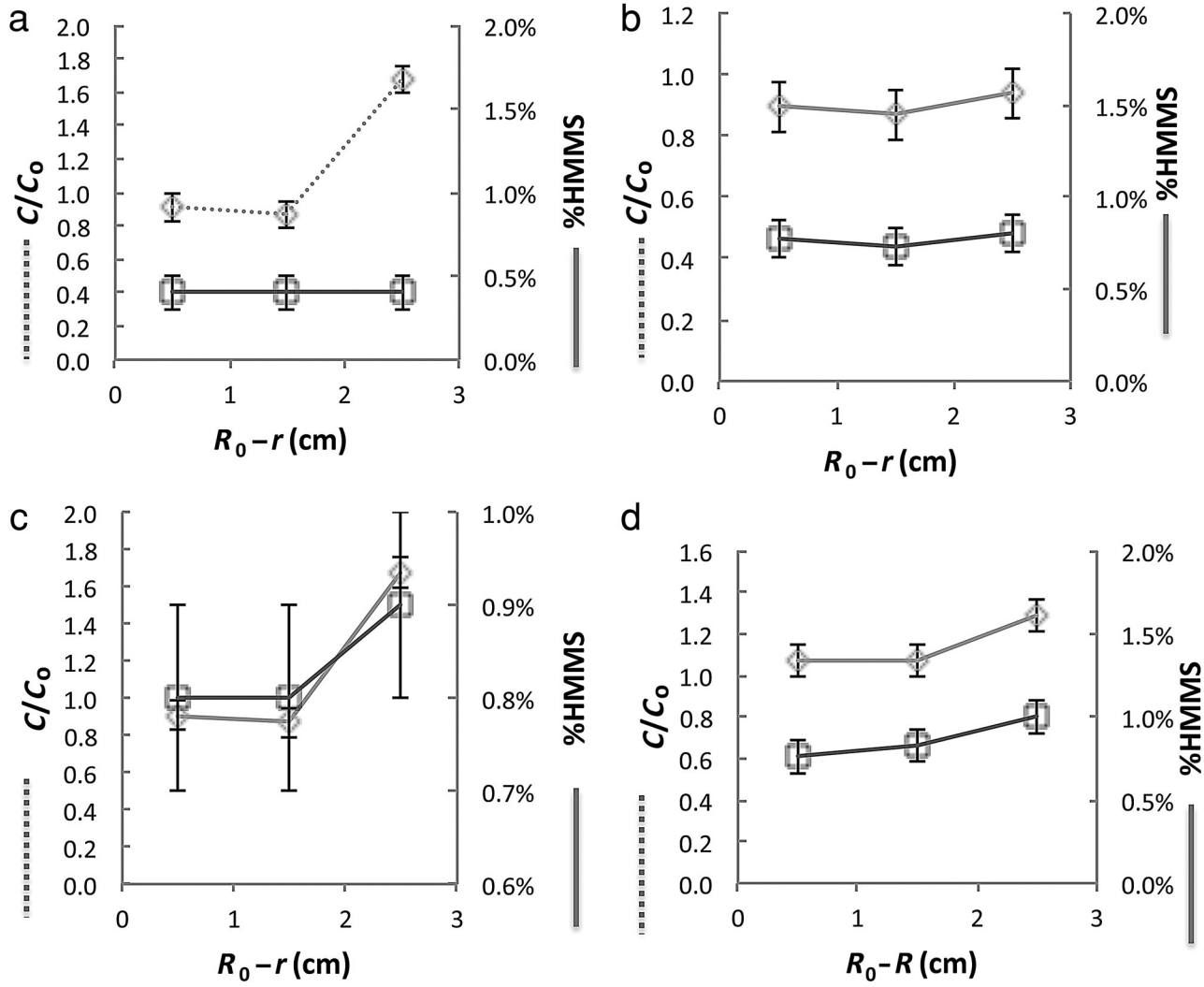


**Figure 3.** Effect of −10°C storage temperature on slow-cooled protein concentration and HMMS. Protein concentration shown is normalized by the initial concentration ($C/C_0$ where $C_0 = 20$ mg/mL), whereas the change in HMMS is shown versus a baseline of 0.4% for stagnant air-cooled samples stored at −10°C. (a) Protein analyzed from the middle slice after storage at −10°C for 70 days. (b) Protein analyzed from the top slice. (c) Middle slice, and (d) bottom slice after storage for 170 days at −10°C.

$C/C_0$, were nearly unity (~0.94–1.05) over all sampling positions in the tank. For the fast cooling rate employed here and for the dimensions of the tank, no significant macroscopic solute polarization was detectable.

Figures 3 and 4 show the concentrations at various locations in the ice (averaged over identical experiments in multiple tanks) for the slow (stagnant air) cooled samples and particular storage times. Concentration polarization at the points near the outer edge of the vessel ($R_0 - r = 0.5$) was small and did not vary significantly with depth (Figs. 3 and 4; Table 1). The middle and bottom slices of the tanks show marked increase in concentration when moving toward the center (at $R_0 - r = 2.5$, $C/C_0$ ~1.3–1.7) (Figs. 3a, 3c, 3d, 4b, and 4c; Table 1). The top slices range from unchanged to lower relative concentration ($C/C_0$ ~0.64–1.08) (Figs. 3b and 4a; Table 1). Within experimental variation, the concentration profiles for the tanks stored at −10°C and −20°C show similar distribution with position, indicating that these profiles are not impacted by long-term storage at these temperatures and are thus a function simply of the initial freezing rate.

### Protein Concentration Profile and Ice Morphology

The exclusion of solutes by the crystallizing water at the onset of freezing results in an increase in solute concentration in the unfrozen solution immediately adjacent to the ice front toward the center of the cylinder. At the same time, the concentration gradient created by the excluded solutes results in diffusion and

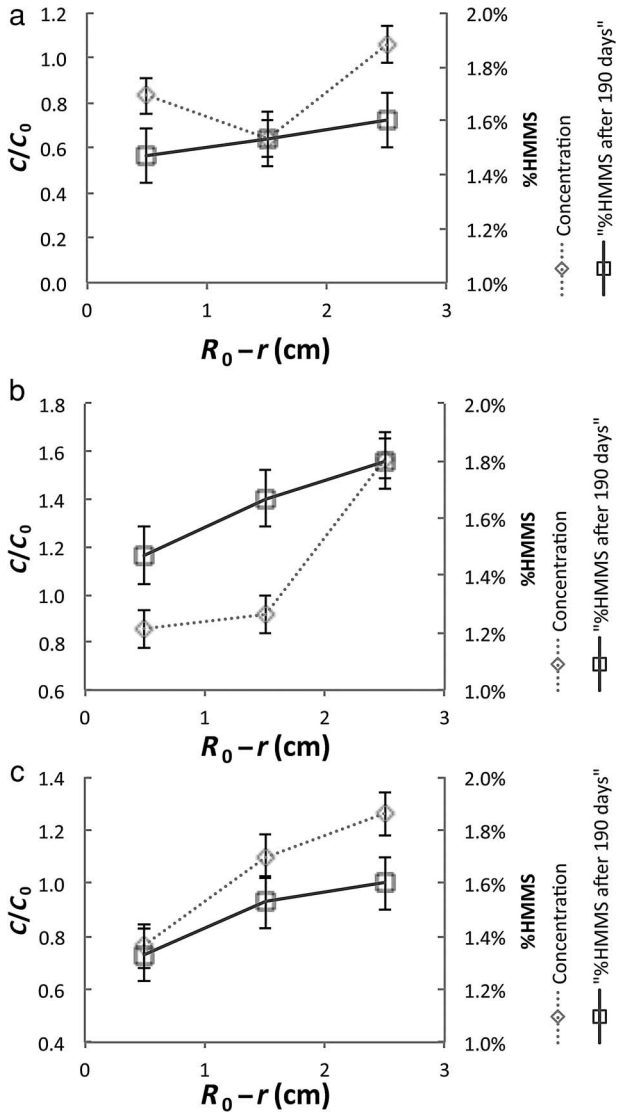


**Figure 4.** Effect of −20°C storage temperature on slow-cooled protein concentration and HMMS. Protein concentration shown is normalized by the initial concentration ($C/C_0$ where $C_0 = 20$ mg/mL), whereas the change in HMMS is shown versus a baseline of 0.4% for stagnant air-cooled samples stored at −10°C. (a) Protein analyzed from the top slice, (b) middle slice, and (c) bottom slice after storage for 190 days at −20°C.

natural convection toward the remaining unfrozen solution, reducing this gradient. The relative rates of the transport away from the interface, along with the natural convection recirculation patterns and the rate of the moving ice front will determine the final concentration profile of solute in the ice.[15,16,29,34] For the liquid-cooled samples, the faster freezing rate and faster ice velocity was found to produce relatively small solute polarization, consistent with our previous report.[19] For the stagnant air-cooled samples, the slower freezing rate allows sufficient time for transport of the solutes away from the ice front, before entrapment in the moving ice front. As the solute concentration (primarily trehalose) increases in the unfrozen liquid adjacent to the ice front, the density of this liquid layer increases, generating a natural convection current. These circulation patterns generate axial gradients in $C/C_0$, increasing $C/C_0$ toward the bottom and center of the tank.[19] Additionally, the minor secondary freezing front in the axial direction resulting from the bottom of the solution directly contacting the stainless steel vessel, whereas the top surface contacts an air space between the solution surface and the stainless steel top, raises $C/C_0$ in the middle versus bottom slice. All freeze-concentration profiles observed in this study agree quite well with those reported previously in Figure 9 of Rodrigues et al.[19] for both rapid and slow freezing. Concentration profiles were measured directly after freezing in the study of Rodrigues et al.,[19] whereas they were measured after specific storage times in the present study.

The concentration polarization behavior shown in Figures 2–4 for the various applied cooling processes is also a consequence of the ice morphology. Differences in ice morphology, particularly the formation of ice dendrites, were previously characterized in terms of the linear ice front velocity.[15,19] A high ice-front velocity due to a faster freezing rate favors nucleation and growth of dendritic ice structures. For example, for BSA and sucrose solutions, a planar ice front was observed for ice front velocities slower than 2 μm/s, whereas above this value instabilities led to dendritic ice fronts.[15,24] Ice dendrites are ice protuberances generated by a supercooled liquid layer immediately ahead of the ice–liquid interface, by either thermal or constitutional supercooling.[16,24] By inhibiting both diffusion and convection in the interdendritic spaces, the formation of dendrites reduces concentration polarization in the solution and therefore in the final solid ice.[15,20,23]

We utilized images of ice structures from our previous study[19] to examine the results of the current study. All of the input conditions and vessels were identical and the measured concentration profiles were essentially the same. The differences in the observed concentration profiles can be explained by the significant differences in the morphological structure of the ice observed for the samples frozen by fast liquid cooling compared with those frozen by slow stagnant air cooling. The ice in the liquid (fast)-cooled stainless steel tank contains well-formed dendrites, as observed experimentally by dyeing the protein with amido black and imaging slices of the ice after freezing.[19] The stained protein gets trapped between the dendrites revealing the structure. In contrast, irregular ice patterns with much less well-developed dendrites, and only near the center, were observed in the stagnant air-cooled tank. Without dendrites,

 DOI 10.1002/jps

**Table 1.** Slow Cooling Effects on Antibody Concentration Within the Vessel*

| Storage Temperature | Number of Tanks | Location of Tank Slice | Outer $C/C_0$ ($R_0 - r = 0.5$) | Middle $C/C_0$ ($R_0 - r = 1.5$) | Center $C/C_0$ ($R_0 - r = 2.5$) |
|---|---|---|---|---|---|
| −10°C | 5 | Top | 0.89 | 0.87 | 0.94 |
| | | Middle | 0.91 | 0.87 | 1.68 |
| | | Bottom | 1.07 | 1.07 | 1.29 |
| −20°C | 1 | Top | 0.83 | 0.64 | 1.06 |
| | | Middle | 0.86 | 0.92 | 1.57 |
| | | Bottom | 0.76 | 1.10 | 1.26 |
| −80°C | 2 | Top | 0.88 | 0.76 | 1.08 |
| | | Middle | 0.86 | 0.78 | 1.55 |
| | | Bottom | 0.73 | 1.04 | 1.45 |

*Value reported is the average concentration measured normalized by the original antibody solution concentration ($C/C_0$ where $C_0 = 20$ mg/mL).

the solute circulating with the natural convection are not trapped as efficiently, resulting in the macroscopic freeze concentration shown in Figures 3–5 and Table 1. However, in the case of fast freezing, dendrite formation occurs almost throughout the entire cross section of the tank.[19] Natural convection currents are inhibited by the dendrites, resulting in the protein and other solutes being trapped in the ice with a relatively smaller polarization or macroscopic cryoconcentration (Fig. 2).

### Structural Changes and Aggregation

Given the above explanation for the observed protein concentration profiles and a mechanism consistent

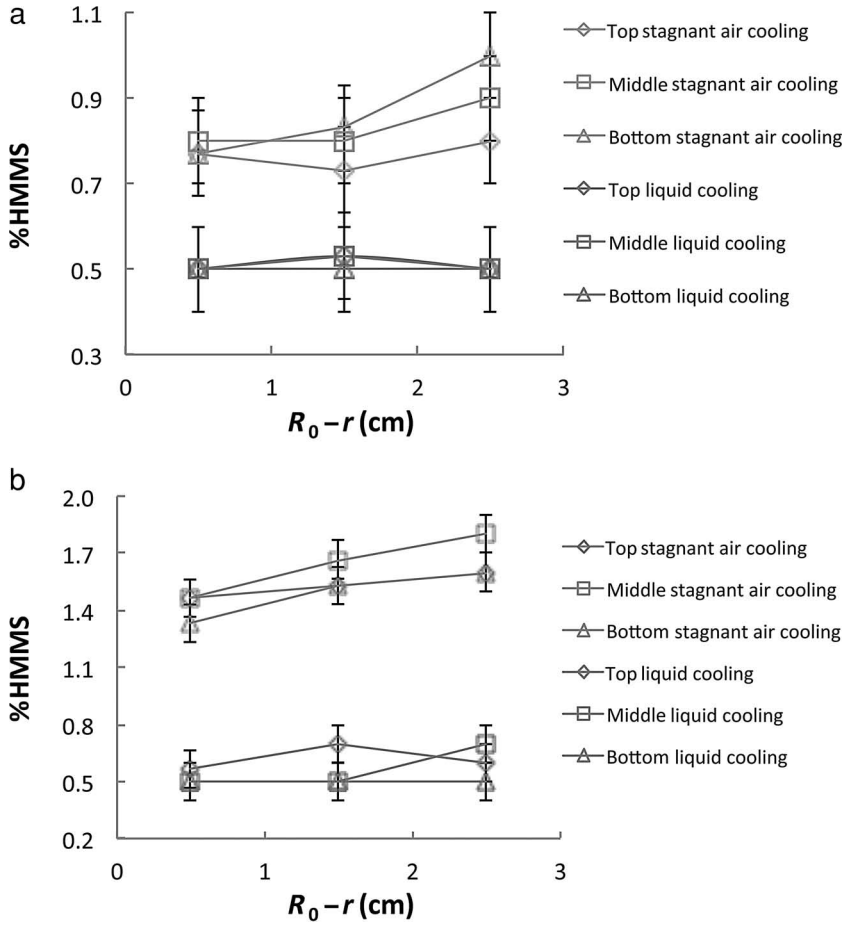


**Figure 5.** Effect of freezing rates and vessel position on HMMS. The %HMMS measured by SEC at different heights and radii by ice sampling after (a) 170 days of storage at −10°C and (b) 190 days of storage at −20°C. Radii measured from the outside to the center of the tank ($R_0 = 2.5$ cm).

**Table 2.** Fast Cooling Effects on Antibody Structure and Activity

| Storage Temperature | # Tanks | Storage Time (days) | Optical Density (350 nm) | Trp Fluorescence ($E_{350}/E_{335}$) | HMMS (%) |
|---|---|---|---|---|---|
| −10°C | 2 | 70 | ND | ND | 0.5 ± 0.1 |
| | 1 | 170 | ND | ND | 0.5 ± 0.1 |
| | 1 | 270 | 0.043 ± 0.004 | 0.853 ± 0.005 | 0.5 ± 0.1 |
| | 1 | 360 | 0.042 ± 0.003 | 0.855 ± 0.004 | 0.5 ± 0.1 |
| −20°C | 1 | 190 | 0.038 ± 0.002 | 0.847 ± 0.005 | 0.6 ± 0.1 |
| | 3 | 230 | 0.042 ± 0.002 | ND | 0.5 ± 0.1 |
| −80°C | 1 | 190 | 0.039 ± 0.001 | 0.856 ± 0.006 | 0.5 ± 0.1 |
| | 1 | 360 | 0.039 ± 0.003 | 0.859 ± 0.005 | 0.5 ± 0.1 |

Average values ± SD reported.

with the results, the main focus of this work is to describe the relationship between these profiles and protein stability. The results are first described in terms of optical density and tryptophan fluorescence, which show an absence of large-scale aggregation. We then describe smaller degrees of aggregation with the more sensitive techniques, namely, SEC.

Data presented in Tables 2 and 3 show that the optical density or turbidity of the samples did not vary significantly with position, time, or freezing rate. Large-protein aggregates were not formed in the study. This agrees with our previous observations with this antibody.[19,25,33] To detect subtle changes in IgG2 conformation after being frozen, stored, and thawed, intrinsic tryptophan fluorescence was used. First, a calibration curve was prepared using IgG2 purposefully denatured with 0–10 M urea and the emission spectra recorded after excitation at 295 nm. Folded protein has a $\lambda_{max}$ of 335 nm, whereas urea denaturation results in a shift in the $\lambda_{max}$ to 350 nm for fully unfolded protein. Notably, the protein is fairly stable, beginning to denature at 5 M urea and completely denaturing in 8 M urea. Second, to use the emission maxima to assess the average-folded state of protein in the ice samples, the ratio of the observed signal intensities at the two wavelengths ($E_{350}/E_{335}$) was recorded. For folded protein in 0 M urea, and until it begins to unfold at ∼5 M urea, a ratio of ∼0.85 is observed. As the protein unfolds, the ratio increases to ∼1.15 (Fig. 1). No changes in $\lambda_{max}$ were detected in any of the frozen samples (data not shown). The $E_{350}/E_{335}$ values (corrected for concentration) for all samples at various storage temperatures and storage times for both freezing rates are unchanged (≈0.85 within experimental error; Tables 2 and 3), similar to the value for properly-folded protein. Therefore, any misfolded protein, if present in the thawed ice core samples, was present at too low a concentration to be detected by this bulk-averaging method. A similar lack of structural changes detectable by intrinsic fluorescence and circular dichroism was reported by Singh et al.[25]

To characterize the protein structure in these samples with greater sensitivity, tryptophan fluorescence signals were used to monitor local structural changes. As a control experiment, incubation with increasing concentrations of urea resulted in a change in tryptophan signal after incubation with ∼5 M urea (Fig. 1). Analysis of the thawed ice core samples showed no significant change in the tryptophan signal for samples that were stagnant air cooled and stored at either −20°C or −10°C and all other samples (Tables 2 and 3).

Aggregation (%HMMS) levels at various positions were quantified by SEC. For storage temperature of −80°C, regardless of cooling rate, the value of %HMMS did not increase over the baseline of ∼0.4%–0.5%, even after 190 or 360 days (Table 2). This indicates that the immediate process of freezing (at any rate) does not in itself lead to the formation of aggregates. When the fast-cooled samples are stored at −10°C, no measurable changes are seen in the aggregation level over relatively long periods of time

**Table 3.** Slow Cooling Effects on Antibody Structure and Activity

| Storage Temperature | # Tanks | Storage Time (Days) | Optical Density (350 nm) | Trp Fluorescence ($E_{350}/E_{335}$) |
|---|---|---|---|---|
| −10°C | 2 | 70 | ND | ND |
| | 1 | 170 | 0.041 ± 0.002 | ND |
| | 1 | 270 | 0.046 ± 0.002 | 0.848 ± 0.005 |
| | 1 | 360 | 0.044 ± 0.003 | 0.857 ± 0.005 |
| −20°C | 1 | 190 | 0.040 ± 0.003 | 0.854 ± 0.003 |
| | 3 | 230 | 0.041 ± 0.002 | ND |
| −80°C | 1 | 190 | 0.039 ± 0.002 | 0.854 ± 0.002 |
| | 1 | 360 | 0.040 ± 0.002 | 0.860 ± 0.006 |

Average values ± SD reported.

(Table 2, Fig. 5a). Slightly greater increases with position are seen in the aggregation levels for fast-cooled samples stored at −20°C, but the changes are deemed to be not significant (Table 2, Fig. 5b).

The storage behavior of the slow-cooled samples is different. At −10°C, small increases in aggregation levels are seen, mainly in the middle and bottom slices toward the center of the tank (Fig. 5a). Although the averages are not impacted significantly (0.4%–0.8%; Table 3), the material at the center (middle and bottom) of the tank does show a greater level of change (to ∼0.8%–1% from ∼0.4%–0.5% initial; Figs. 3c, 3d, and 5a). Material in the top slice shows greater stability (Figs. 3a, 3b, and 5a).

On the contrary, the slow-cooled samples stored at −20°C show more significant increases in aggregation in all positions (Figs. 4a–4c and 5b) ranging between ∼0.9% and 1.4% from the initial ∼0.4%–0.5%. Aggregation levels in the top slice had the least positional dependence, whereas the middle slice had the most, in line with the corresponding concentration differential across the radius of the tank. The average aggregation level was ∼1.5% at day 190 and ∼2% at day 230 (data not shown).

After 70 days of storage at −10°C, for the core samples at all locations within the vessel, regardless of freezing rate, a baseline level of ∼0.4%–0.5% HMMS was detected, similar to that observed for never frozen control protein and likely because of the protein handling steps (thawing and shipping) before analysis (Figs. 3 and 4).[23] After 170 days of storage at −10°C, a slight difference in percentage of HMMS between the slow and fast freezing rates appeared. For the samples frozen by fast liquid cooling, the HMMS values remained ∼0.4%–0.5% (Table 2) but were approximately twofold larger for the samples frozen by slow stagnant air cooling, ∼0.8%–1% (Fig. 5a). These levels are just slightly higher than the significant difference level by the SEC method of ∼0.2%. For slow cooling, a higher HMMS was observed toward the center of the tank ($R_0 - r = 2.5$) versus the outside of the tank ($R_0 - r = 0.5$), especially for the middle and bottom slices (Figs. 3c and 3d). For samples stored for 190 days at −20°C, the difference in %HMMS with freezing rate was accentuated even further (Fig. 5b). Again, for the liquid-cooled sample, there was a negligible change in the %HMMS at all points measured throughout the tank. On the contrary, for the stagnant air-cooled samples, the average %HMMS was significantly higher, ∼1.5%. For the top slice, the change in %HMMS with radius was slight, whereas for the bottom and middle slices, a relatively linear increase in %HMMS was observed for the samples measured from the outside to the center of the tank (Figs. 4b, 4c, and 5b). For slowly frozen samples stored in three separate vessels at −20°C for 230 days and thawed as a single bulk without slicing or sampling, a similar high %HMMS of ∼1.9% was measured. With a storage temperature of −80°C, regardless of cooling rate, the value of %HMMS did not increase over the baseline of ∼0.4%–0.5%, even after 190 or 360 days (Table 2).

## DISCUSSION

In our earlier studies, we have elucidated the impact of cooling rate on concentration gradients and ice morphology[19] and the impact of long-term frozen-state storage temperature on aggregation of the IgG2 mAb.[25] In this study, we attempt to deconvolute the impact of the process parameter (cooling rate) and the resulting solute polarization and ice morphology on the long-term storage behavior. The results discussed above clearly show that dependence exists between the two.

The results, in summary, show that solute polarization occurs in the tanks as the tanks are cooled and frozen as measured by the ice coring. Slow cooling (∼220 min in stagnant air) leads to a greater degree of difference between outer edges of the tank and the center with higher concentrations of solutes in the middle and bottom layers, whereas the top layer is slightly depleted. Fast cooling (∼25 min in liquid coolant) leads to much smaller differences in the distribution of solutes over the tank. Surprisingly, differences in aggregation behavior are seen with the cooling rate on placing these tanks on stability at −10°C and −20°C (above $T'_g$). No large particulate aggregates were seen in any system. Fast-cooled tanks show small to no increase in aggregation (reported as %HMMS by SEC-HPLC) in any position in the tank with time at any storage temperature. Slow-cooled tanks show no change in aggregation at any position when stored at −80°C (below $T'_g$). However, when stored at −10°C or −20°C, increases in aggregation are measured overtime. These increases are smaller at −10°C compared with −20°C. In both cases, the increase in aggregation at any position generally parallels the (increase in) solute–protein concentration mentioned above.

Table 4 provides an overall qualitative summary of the observations in this report, correlating processing rate and storage temperature to aggregation behavior on long-term storage. Aggregation in the frozen state requires two conditions to be fulfilled. First is the formation and persistence of aggregation-competent denatured or partially misfolded species. Second is the requirement of (a) mobility and (b) the opportunity for these aggregation-competent species to interact with nearest neighbors to actually form aggregates. The first condition is determined by the process, whereas the outcome of the second is determined by the storage condition. Outcome of storage below $T'_g$ is independent of processing rate. However, the observation

**Table 4.** Summary of Protein Stability as Impacted by Freezing Rates and Storage Temperature

| | Storage Temperature | |
|---|---|---|
| | $<T'_g$ | $>T'_g$ |
| Slow freezing | +++ | + |
| Fast freezing | +++ | +++ |

+++, no; ++, minimal; +, some detectable HMMS or loss of native structure.

that process rate can lead to different outcomes for storage temperature above $T'_g$ suggests a more complex behavior.

We note that simple freeze and thaw of this IgG2 in the trehalose formulation does not lead to aggregation detectable by SEC.[18,27] Thus, any aggregation-competent species formed during the processing (irrespective of rate) will not aggregate, if not given adequate time (of the order of months). Even in this study, for the stagnant air-cooled samples stored at −10°C, there was no change in %HMMS after 70 days in the center slice (Fig. 3a) at all radial locations, indicating that aggregates were not produced during the freezing or thawing processes.

The lack of aggregation on storage at −80°C, well below the $T'_g$, is simply explained by lack of mobility. The $T'_g$ of this IgG2 formulation with trehalose was experimentally verified by differential scanning calorimetry to be between −29°C and −30°C (results not shown). The lack of observed changes in Trp fluorescence and the lack of aggregates by $A_{350}$ and SEC after even after one year at −80°C indicate that any aggregation-competent species formed during freezing were reversible and simply reverted to the native state upon thawing. This lack of aggregates was observed even for slowly frozen samples with large freeze concentration $C/C_0$ values, indicating that when below $T'_g$, the storage temperature determines the outcome and not the process conditions.

On the contrary, for storage above $T'_g$ (−20°C and −10°C), the impact of process conditions on change in %HMMS was significant for all locations (Fig. 5). Fast cooling led to small radial differences in $C/C_0$ and unchanged %HMMS (Figs. 2 and 5). However, even when the $C/C_0$ was below or near unity, a large increase in %HMMS was present for slow cooling rates (Figs. 3 and 4). A key difference between fast and slow freezing was that the time to reach −20°C was 25 min for the liquid-cooled sample and 220 min for the stagnant air-cooled sample and reference.[19] As discussed above, fast cooling also resulted in formation of dendrites through almost the entire cross section of the vessel unlike with slow cooling.

A variety of factors will impact the formation of aggregation-competent species during the freezing process. Exposure of protein molecules to the ice–liquid interface can result in their denaturation.[35–38] Also, during freezing, the protein molecules in the unfrozen liquid phase are exposed to potentially destabilizing environment of increasing ionic strength, changes in pH, as well as increasing protein concentration.[14,39] Protein molecules trapped in regions apart from the FCM are also subject to dehydration stress.[21] The phenomena of cold denaturation also results in unfolding of protein.[14] The cold denaturation temperature for an IgG1 has been reported to be −23°C[40] and is likely to be similar for an IgG2; however, cold denaturation-induced unfolding in this system in the presence of ice is not expected to be relevant. Total protein exposure to the ice–liquid interface depends upon the time of exposure and the surface area of the interface. For fast freezing with prevalent dendrites, the ice–liquid interfacial area (due to the dendrites) is larger than for slow freezing. It is thus likely that denatured species due to the interface are more numerous after fast freezing than slow. On the contrary, the exposure time to destabilizing conditions is much less during faster freezing (25 vs. 220 min). It is thus possible that during the fast freezing, a smaller fraction of the protein in FCM (i.e., protein not in contact with the interface) in a given volume is destabilized compared with slow freezing. Because slow freezing leads to a greater proportion of total protein being in the FCM phase, the overall proportion of destabilized molecules (interface + FCM) may be higher after slow freezing. Although the relative contribution of these individual factors cannot be deconvoluted, fast freezing may lead to a smaller proportion of aggregation-competent species being generated at the end of the freezing process, relative to slow freezing.[14] This reflects the contribution of the process conditions, as required above. Dong et al.[21] also found lower hydration levels for lysozyme in the FCM for their slow crystal growth (low supercooling) sample compared with the sample with rapid crystal formation (high supercooling). This would potentially reduce the stability of lysozyme in the FCM of what would be equivalent of a slow-frozen sample.

When these two sets of samples are subsequently stored above $T'_g$ and under appropriate conditions, slow-frozen systems with its greater proportion of aggregation-competent species will show a higher rate of aggregation overtime. The rate would also be likely enhanced by the higher $C/C_0$ in the slow-frozen system with more protein molecules in close proximity. Storage above $T'_g$ allows mobility; thus, fulfilling one requirement (a), of the storage condition. However, the second requirement (b), the opportunity, for aggregation-competent species to aggregate on storage above $T'_g$ is created by the ability of trehalose to crystallize at these temperatures.[41] Crystallization of trehalose leads to loss of cryoprotectant, allowing the aggregation-competent protein molecules to

interact with nearest neighbors. This interaction is facilitated by the enhanced mobility above $T'_g$. The aggregation behavior seen here for the slow-frozen material stored at −10°C and −20°C broadly agrees with the observations reported in Singh et al.,[25] where significant aggregation was observed at −20°C, whereas limited to none at −10°C. With increased mobility, aggregation-competent molecules can either interact with neighbors to aggregate or refold and thus not aggregate. The balance of these two protein processes in the absence of cryoprotection, leads to increase in aggregation at −20°C and much lower aggregation at −10°C.[25]

With regard to the importance of a stable amorphous cryoprotectant, it is worth noting that as proposed in Singh et al.,[25] the use of the noncrystallizing cryoprotectant sucrose has enabled a number of molecules to be stored above $T'_g$ for a number of years (data not shown). Other case studies have been reported on the importance of the cryoprotectant remaining in the amorphous state after freezing to prevent aggregation.[42,43]

Interestingly, the lack of aggregation seen for fast-frozen systems in this work, despite storage above $T'_g$, suggests that the interplay between process rate and storage conditions is more complex. One possibility is that there simply are not enough aggregation-competent species after fast freezing, to result in measurable aggregation. A second possible explanation could be that the interdendritic spaces in which the solutes (trehalose, buffer, and protein) are trapped are small with a better intermingling of the solute molecules. Faster cooling prevents the faster migrating solutes (e.g., trehalose) from separating from the slower migrating protein. The resultant intimate mixture may prevent the trehalose from crystallizing. The small interdendritic space bounded by ice may also restrict the growth of any trehalose crystals that are formed. A significant portion of the protein thus retains its cryoprotectant and therefore does not aggregate. The intimate mixing with solute trehalose also means that the protein molecules are better separated from each other. This would also prevent aggregation, and even if aggregates are formed the small amount of protein in the impacted space would prevent the aggregates from involving any significant amount of protein. Analogously, with slow cooling, the lack of well-formed dendrites allows larger pockets of solutes to be created. Crystals of trehalose in these pockets could grow larger and thus deprive a greater number of protein molecules from cryoprotectant. Further work is needed to elucidate this mechanism in greater detail.

Finally, the authors′ would like to note that although the formation of denatured or partially misfolded molecules at the ice interface has been well documented,[44,45] aggregation of proteins is known to occur through native-state associations also. It, therefore, cannot be ruled out that such associations contribute to the aggregation in the frozen system also, although we expect the contribution to be small because of the reasons given below. (1) Such native-state association would have to occur away from the interface (i.e., in the FCM). A large fraction of the total protein is actually captured in the FCM compared with the interface, implying that if native-state association was a prominent route of aggregation, it would be expected to lead to a higher level of aggregation than observed. (2) The trehalose also concentrates significantly in the FCM and would tend to reduce the tendency for such self-association because of its significantly higher molar concentration compared with the protein.

### Other Modes of Rapid Protein Freezing

The faster freezing rate produced by liquid cooling the 50 mL vessels prevented a detectable change in protein aggregation. However, extremely fast freezing by liquid nitrogen can, in some cases, cause aggregation and denaturation of proteins.[46] The submersion of small containers with ~1–2 mL of protein solution into liquid nitrogen can cause the formation of soluble and insoluble protein aggregates and loss of biological activity measured upon melting.[40,47] This destabilization has been attributed to interactions of protein with high ice–liquid interfacial area from significant ice nucleation without the use of appropriate cryoprotectants.[6] However, other rapid freezing techniques, including spray freeze drying,[37,48] spray freezing into liquids,[49,50] thin film freezing,[51] and spiral wound *in situ* freezing[52] produce stable protein by limiting the exposure to destabilizing ice–liquid interfaces with appropriate cryoprotectants such as trehalose, and by controlling the area of the air–liquid interface.[49–52] In the present study, the faster freezing rate was orders of magnitude slower, and thus, the areas of the ice–liquid and air–liquid interfaces were much smaller.

### Implications on Industrial Scale Frozen Protein Storage

Although 50 mL tanks were used in this study with a well-defined geometry, larger tanks up to 300 L are of interest on an industrial scale.[23,27] Large tanks will perforce be cooled slowly with process times of up to 12 h.[26,29] The study shows that process conditions in small-scale vessels can impact the outcome on long-term storage. As these vessels are generally used to mimic the large-scale vessels, a better representation may be obtained by slow-cooling the small vessels also.

The safest long-term storage temperature in all cases is below the $T'_g$ of the formulation. This is particularly true for formulations where the

cryoprotectant has a tendency to crystallize (e.g., trehalose, sorbitol, and mannitol).[25,42,43] High protein concentrations will help to raise the $T'_g$. Because a decrease in the storage temperature for large-scale tanks dramatically increases the cost of storage, reducing concentration polarization by increasing the freezing rate and enabling formation of dendrites would be desirable. In large tanks, internal cooling surfaces would be required to decrease heat and mass transfer dimensions and to supplement cooling from the outer wall. For example, fins and baffles are utilized to decrease natural convection and diffusion toward the center of the larger tanks.[20] The additional cooling surfaces have been shown to enhance formation of dendritic ice on a large scale.[23] Honeycomb-like geometries would be better but technically complicated to produce and use.

## CONCLUSIONS

We have shown that freezing protein solutions containing a cryoprotectant in small cylindrical vessels results in differences in the macroscopic solute distribution or polarization that is a function of the processing conditions. Fast cooling that leads to the formation of ice dendrites results in entrapment of the solutes in the interdendritic spaces and therefore a more uniform distribution of solutes throughout the geometry of the tank. Slow cooling does not enable these dendrites until a significant portion of the material is frozen. A greater degree of solute polarization is therefore seen in these vessels, with solutes driven by diffusive and convective transport toward the middle and bottom positions.

In the case of the IgG2 mAb used in this study, the process of freezing itself does not generate permanently misfolded species, as seen when tanks (fast or slow frozen) stored at $-80^\circ$C (below $T'_g$) are thawed. Fast-frozen tanks, when stored at either $-10^\circ$C or $-20^\circ$C (above $T'_g$), also show no change in aggregation levels overtime. On the contrary, slow-frozen tanks when stored at either $-10^\circ$C or $-20^\circ$C show increase in aggregation levels overtime and the presence of misfolded species on thawing.

Our earlier work demonstrated that long-term outcome of frozen storage in a trehalose formulation is dependent on the storage temperature vis a vis the $T'_g$ as a consequence of processes that are triggered by mobility above $T'_g$—trehalose crystallization, protein aggregation, and protein refolding.[25] The current work now shows that the nature of the ice and solute distribution also determines the outcome of long-term storage even above $T'_g$.

Taken together, protein aggregation in the current trehalose system appears to correlate with: (1) amount of aggregation-competent species generated due to the denaturation at ice–liquid interface and to the exposure time of the protein to the destabilizing stresses in solution while in the highly concentrated unfrozen state. (2) The storage temperature that allows the cryoprotectant to crystallize thus providing the mobility and opportunity for the aggregation-competent species to interact with nearest neighbors and aggregate. (3) The distribution of solutes including protein in the interdendritic spaces. The presence of ice dendrites in the fast-frozen tanks distributes the solutes more uniformly in smaller interdendritic regions. A hypothesis for the observed impact of processing conditions on outcome of long-term storage has been provided.

This study for the first time has shown the direct importance processing conditions on the stability of protein during long-term-frozen storage. Large commercial tanks are slow-cooled systems and thus this study underscores the importance of processing parameters and storage conditions on the viability of long-term protein storage, especially with excipients that could crystallize. Although our work shows that freezing rate compensates for excipient crystallization (at least with trehalose) during frozen storage in the small-scale systems, we caution against the use of this observation in a general sense until it has been studied further and understood. It is safer to place proteins with crystallization-prone cryoprotectants (e.g., trehalose and sorbitol) under $T'_g$ for long-term storage.

The study also shows how small-scale models can be used to provide a greater degree of resolution about the processes occurring in large-scale tanks. It is general practice that such small tanks are simply placed in the freezer and used as stability models with each data/time point represented by an individual tank. Our study shows that greater care is required to make these models representative of full scale. We believe that such fundamental understanding of factors contributing to protein aggregation during freezing and storage in the simple geometry of small cylindrical tanks will aid in design of large-scale commercial tanks and the engineering challenges in freezing rate control.

## ACKNOWLEDGMENTS

The authors would like to acknowledge Pfizer for the financial support as well as for the supply of protein for this project. This work was also supported by grants from the Welch Foundation (F-1319 to K.P.J. and F-1767 to J.A.M.) and the Portuguese Foundation for Science and Technology (PTDC/EQU-EQU/104318/2008 to M.A.R.).

## REFERENCES


1. Nelson AL, Dhimolea E, Reichert JM. 2010. Development trends for human monoclonal antibody therapeutics. Nat Rev Drug Discov 9:767–774.
2. Sheridan C. 2010. Fresh from the biologic pipeline-2009. Nat Biotechnol 28(4):307–310.
3. Kelley B. 2009. Industrialization of mAb production technology: The bioprocessing industry at a crossroads. MAbs 1(5):443–452.
4. Singh S, Kolhe P, Nema S, Wang W. 2009. Large-scale freezing of biologics—A practitioner's review. Part I fundamental aspects. BioProcess Int 7(9):32–44.
5. Webb SD, Webb JN, Hughes TG, Sesin DF, Kincaid AC. 2002. Freezing biopharmaceuticals using common techniques—and the magnitude of bulk-scale freeze-concentration. BioPharm 15(5):22–34.
6. Strambini G, Gabellieri E. 1996. Proteins in frozen solutions: Evidence of ice-induced partial unfolding. Biophys J 70:971–976.
7. Kueltzo LA, Wang W, Randolph TW, Carpenter JF. 2007. Effects of solution conditions, processing parameters and container materials on aggregation of a monoclonal antibody during freeze-thawing. J Pharm Sci 97(5):1801–1812.
8. Carpenter JF, Izutsu K-I, Randolph TW. 2004. Freezing and drying induced perturbations of protein structure and mechanisms of protein protection by stabilizing additives. In Freeze drying/lyophilization of pharmaceutical and biological products; Rey L, May JC, Eds. New York: Marcel Dekker, Inc., pp 147–186.
9. Avastin: EPAR Scientific Discussion. 2006. Accessed 02/01/2013, at: http://www.emaeuropaeu/docs/en_GB/document_library/EPAR_-_Scientific_Discussion/human/000582/WC500029262.pdf, ed.
10. Shamlou PA, Breen LH, Bell WV, Pollo M, Thomas BA. 2007. A new scaleable freeze-thaw technology for bulk protein solutions. Biotechnol Appl Biochem 46:13–26.
11. Pikal MJ, Dellerman KM, Roy ML, Riggin RM. 1991. The effects of formulation variables on the stability of freeze-dried human growth hormone. Pharm Res 8(4):427–436.
12. Sarciaux J-M, Mansour S, Hageman MJ, Nail SL. 1999. Effects of buffer composition and processing conditions on aggregation of bovine IgG during freeze-drying. J Pharm Sci 88(12):1354–1361.
13. Pikal-Cleland KA, Rodriguez-Hornedo N, Amidon GL, Carpenter JF. 2000. Protein denaturation during freezing and thawing in phosphate buffer systems: Monomeric and tetrameric beta-galactosidase. Arch Biochem Biophys 384(2):398–406.
14. Bhatnagar BS, Bogner RH, Pikal MJ. 2007. Protein stability during freezing: Separation of stresses and mechanisms of protein stabilization. Pharm Dev Technol 12(5):505–523.
15. Butler MF. 2002. Freeze concentration of solutes at the ice/solution interface studied by optical interferometry. Cryst Growth Des 2(6):541–548.
16. Korber C. 1988. Phenomena at the advancing ice-liquid interface: Solutes, particles and biological cells. Q Rev Biophys 21(2):229–298.
17. Chen YH, Cao E, Cui ZF. 2001. An experimental study of freeze concentration in biological media. Food Bioproducts Process 79(1):35–40.
18. Ayel V, Lottin O, Faucheux M, Sallier D, Peerhossainni H. 2006. Crystallization of undercooled aqueous solutions: Experimental study of free dendritic growth in cylindrical geometry. Int J Heat Mass Transf 49:1876.
19. Rodrigues MA, Miller MA, Glass MA, Singh SK, Johnston KP. 2011. Effect of freezing rate and dendritic ice formation on concentration profiles of proteins frozen in cylindrical vessels. J Pharm Sci 100(4):1316–1329.
20. Wilkins J, Sesin D, Wisniewski R. 2001. Large-scale cryopreservation of biotherapeutic products. Innov Pharm Technol 1(8):174–180.
21. Dong J, Hubel A, Bischof JC, Aksan A. 2009. Freezing-induced phase separation and spatial microheterogeneity in protein solutions. J Phys Chem B 113(30):10081–10087.
22. Miyawaki O, Liu L, Nakamura K. 1998. Effective partition constant of solute between ice and liquid phases in progressive freeze-concentration. J Food Sci 63:756–758.
23. Wisniewski R, Wu V. 1996. Large-scale freezing and thawing of biopharmaceutical products. In Biotechnology and Biopharmaceutical Manufacturing, Processing Preservation, Avis, EA and Wu V, Eds. CRC Press (Boca Raton, Florida), pp 7–59.
24. Butler MF. 2000. Instability formation and directional dendritic growth of ice studied by optical interferometry. Cryst Growth Des 1(3):213.
25. Singh SK, Kolhe P, Mehta AP, Chico SC, Lary AL, Huang M. 2011. Frozen state storage instability of a monoclonal antibody: Aggregation as a consequence of trehalose crystallization and protein unfolding. Pharm Res 28(4):873–885.
26. Singh S, Kolhe P, Nema S, Wang W. 2009. Large-scale freezing of biologics—A practitioner's review. Part II: Practical advice. BioProcess Int 7(10):34–42.
27. Singh S. 2007. Storage consideration as part of the formulation development program for biologics. Am Pharm Rev 10(3):26–33.
28. Singh S, Kolhe P, Wang W, Nema S. 2009. Large-scale freezing of biologics—A practitioner's view. Part II: Practical advice. BioProcess Int 7(10):34–42.
29. Kolhe P, Amend E, Singh SK. 2010. Impact of freezing on pH of buffered solutions and consequences for monoclonal antibody aggregation. Biotechnol Prog 26(3):727–733.
30. Roos Y, Karel M. 1991. Applying state diagrams to food processing and development. Food Technol 45(12):66, 68–71, 107.
31. Garidel P, Hegyi M, Bassarab S, Weichel M. 2008. A rapid, sensitive and economical assessment of monoclonal antibody conformational stability by intrinsic tryptophan fluorescence spectroscopy. Biotechnol J 3:1201–1211.
32. Walton TA, Sousa MC. 2004. Crystal structure of Skp, a prefoldin-like chaperone that protects soluble and membrane proteins from aggregation. Mol Cell 15(3):367–374.
33. Barnard JG, Singh S, Randolph TW, Carpenter JF. 2011. Subvisible particle counting provides a sensitive method of detecting and quantifying aggregation of monoclonal antibody caused by freeze-thawing: Insights into the roles of particles in the protein aggregation pathway. J Pharm Sci 100(2):492–503.
34. Gu X, Suzuki T, Miyawaki O. 2005. Limiting partition coefficient in progressive freeze-concentration. J Food Sci 70(9):546–551.
35. Carpenter JF, Chang BS, Randolph TW. 2004. Physical damage to proteins during freezing, drying, and rehydration. In Lyophilization of biopharmaceuticals; Costantino HR, Pikal MJ, Eds. AAPS Press (Arlington, Virginia), pp 423–442.
36. Webb SD, Cleland JL, Carpenter JF, Randolph TW. 2003. Effects of annealing lyophilized and spray-lyophilized formulations of recombinant human interferon-γ. J Pharm Sci 92(4):715–729.
37. Maa Y-F, Prestrelski SJ. 2000. Biopharmaceutical powders: Particle formation and formulation considerations. Curr Pharm Biotechnol 1:283–302.
38. Pikal-Cleland KA, Cleland JL, Anchordoquy TJ, Carpenter JF. 2002. Effect of glycine on pH changes and protein stability during freeze-thawing in phosphate buffer systems. J Pharm Sci 91(9):1969–1979.
39. Timasheff SN. 1992. Stabilization of protein structure by solvent additives. In Stability of protein pharmaceuticals: Part B; Ahern TJ, Manning MC, Eds. Springer (New York, New York). pp 265–285.

40. Chang BS, Kendrick BS, Carpenter JF. 1996. Surface-induced denaturation of proteins during freezing and its inhibition by surfactants. J Pharm Sci 85(12):1325–1330.
41. Sundaramurthi P, Suryanarayanan R. 2010. Trehalose crystallization during freeze-drying: Implications on lyoprotection. J Phys Chem Lett 1:510–514.
42. Piedmonte DM, Summers C, McAuley A, Karamujic L, Ratnaswamy G. 2007. Sorbitol crystallization can lead to protein aggregation in frozen protein formulations. Pharm Res 24(1):136–146.
43. Zhou R, Schlam RF, Yin S, Gandhi RB, Adams ML. 2010. Scale considerations for selection of saccharide excipients for liquid formulations. J Pharm Sci 100(4):1605–1606.
44. Strambini GB, Gabellieri E. 1996. Proteins in frozen solutions: Evidence of ice-induced partial unfolding. Biophys J 70(2):971–976.
45. Schwegman JJ, Carpenter JF, Nail SL. 2009. Evidence of partial unfolding of proteins at the ice/freeze-concentrate interface by infrared microscopy. J Pharm Sci 98(9):3239–3246.
46. Strambini GB, Gonnelli M. 2007. Protein stability in ice. Biophys J 92:2131–2138.
47. Jiang S, Nail SL. 1998. Effect of process conditions on recovery of protein activity after freezing and freeze-drying. Eur J Pharm Biopharm 45(3):249–257.
48. Webb SD, Cleland JL, Carpenter JF, Randolph TW. 2002. A new mechanism for decreasing aggregation of recombinant human interferon-gamma by a surfactant: Slowed dissolution of lyophilized formulations in a solution containing 0.03% polysorbate 20. J Pharm Sci 91(2):543–558.
49. Engstrom JD, Simpson DT, Cloonan C, Lai ES, Williams III RO, Kitto GB, Johnston KP. 2007. Stable high surface area lactate dehydrogenase particles produced by spray freezing into liquid nitrogen. Eur J Pharm Biopharm 65:163–174.
50. Engstrom JD, Simpson DT, Lai ES, Williams III RO, Johnston KP. 2007. Morphology of protein particles produced by spray freezing of concentrated solutions. Eur J Pharm Biopharm 65:149–162.
51. Engstrom JD, Lai ES, Ludher BS, Chen B, Milner TE, Williams III RO, Kitto GB, Johnston KP. 2008. Formation of stable submicron protein particles by thin film freezing. Pharm Res 25(6):1334–1346.
52. Miller MA, Khan TA, Kaczorowski KJ, Wilson BK, Dinin AK, Rodrigues MA, Johnston KP, Maynard JA. 2012. Antibody nanoparticle dispersions formed with mixtures of crowding molecules retain activity and in vivo bioavailability. J Pharm Sci 101:3763–3778.